mixture was concentrated on a rotary evaporator and chromatographed on a silica gel column (hexane/ether = 10:1 to 5:1) to give 80 mg (51%) of chalcone.

Registry No. **1a**, 75-97-8; **1b**, 98-86-2; **1c**, 96-22-0; **1d**, 93-55-0; **1e**, 120-92-3; **1f**, 108-94-1; **2a**, 110614-54-5; **2b**, 41492-37-9; **2c**, 110614-55-6; **2d**, 110614-56-7; **2e**, 110614-57-8; **2f**, 110614-58-9; **3a**, 110614-59-0; **3b**, 41492-33-5; **3c**, 110614-60-3; **3d**, 110614-61-4; **3e**, 110614-62-5; **3f**, 110614-63-6; **4a**, 110614-64-7; **4b**, 38860-13-8; Me_3GeCl, 1529-47-1; benzaldehyde, 100-52-7; chalcone, 94-41-7.

Stereochemical and Electrochemical Characterization of the Iron–Iron Multiple-Bonded $[Fe_2(\eta^5\text{-}C_5H_{5-x}Me_x)_2(\mu\text{-}NO)_2]^n$ Dimers (x = 0, 1, 5; n = 0, 1–): A Structural-Bonding Analysis of the Iron and Cobalt Nitrosyl-Bridged $[M_2(\eta^5\text{-}C_5H_5)_2(\mu\text{-}NO)_2]^n$ Series (M = Fe, n = 0, 1–; M = Co, n = 1+, 0)

Kimberly A. Kubat-Martin,[1a] Mary E. Barr, Brock Spencer,[1b] and Lawrence F. Dahl*

Department of Chemistry, University of Wisconsin—Madison, Madison, Wisconsin 53706

Received June 11, 1986

In connection with our previous investigations of the 32/33-electron $[Co_2(\eta^5\text{-}C_5R_5)_2(\mu\text{-}CO)_2]^n$ series (n = 0, 1–), we have carried out structural-bonding studies of the 32-electron $Fe_2(\eta^5\text{-}C_5H_{5-x}Me_x)_2(\mu\text{-}NO)_2$ dimers (x = 0, 1, 5) and the 33-electron $[Co_2(\eta^5\text{-}C_5H_4Me)_2(\mu\text{-}NO)_2]^+$ monocation. The results reported herein include the following: (1) Cyclic voltammetric measurements showed that the three neutral iron dimers undergo similar one-electron reversible reductions to their respective monoanions. The $E_{1/2}$ values exhibit a linear change in negative voltage per methyl ring substituent consistent with increased difficulty in reduction upon methyl ring substitution. (2) An X-ray crystallographic determination of the 32-electron $Fe_2(\eta^5\text{-}C_5H_4Me)_2(\mu\text{-}NO)_2$ disclosed a planar $Fe_2(NO)_2$ core of crystallographic C_{2h}—2/m site symmetry with an Fe–Fe distance of 2.326 (4) Å which is identical with that in the previously characterized $Fe_2(\eta^5\text{-}C_5H_5)_2(\mu\text{-}NO)_2$. (3) An X-ray crystallographic determination of the 33-electron $[Fe_2(\eta^5\text{-}C_5H_5)_2(\mu\text{-}NO)_2]^-$ monoanion (isolated as the $[PPN]^+$ salt) showed that the salient geometrical change resulting from the oxidation of the monoanion to its 32-electron neutral parent is a decrease in the Fe–Fe distance from 2.378 (1) (av) to 2.326 (4) Å. This 0.052-Å shortening in the metal–metal distance (upon oxidation) is completely compatible with the unpaired electron in the monoanion occupying a HOMO mainly composed of out-of-plane d_π dimetal-antibonding character. This geometrical change provides an experimental operational test that the isoelectronic $[Fe_2(\eta^5\text{-}C_5R_5)_2(\mu\text{-}NO)_2]^n$ and $[Co_2(\eta^5\text{-}C_5R_5)_2(\mu\text{-}CO)_2]^n$ series (n = 0, 1–) have similar corresponding LUMO's (n = 0) and HOMO's (n = 1–). (4) In light of the previously reported (and theoretically inexplicable) bond-length decrease of 0.05 Å in the mean Co–NO distance upon oxidation of the 34-electron $Co_2(\eta^5\text{-}C_5H_5)_2(\mu\text{-}NO)_2$ neutral parent to its 33-electron monocation, a crystallographic determination of the corresponding $[Co_2(\eta^5\text{-}C_5H_4Me)_2(\mu\text{-}NO)_2]^+$ monocation (isolated as the $[PF_6]^-$ salt) was performed. An examination of the centrosymmetric $Co_2(NO)_2$ cores in these C_5H_4Me- and C_5H_5-containing dimers revealed abnormally elongated out-of-plane thermal ellipsoids for the nitrogen and oxygen atoms in both monocations. We propose that the similarly short mean Co–NO bond lengths in these monocations are due in large part to an artifact of crystal disorders involving a superposition of at least two nonplanar orientations for each nitrosyl ligand; hence, the *actual* Co–NO bond lengths in these cobalt monocations may *not* be smaller than those in their neutral parents. $Fe_2(\eta^5\text{-}C_5H_4Me)_2(\mu\text{-}NO)_2$: M_r 329.95; monoclinic; $C2/m$; a = 7.966 (4) Å, b = 8.644 (2) Å, c = 9.833 (4) Å, β = 113.36 (3)°, V = 621.6 (4) Å^3 at T = 233 K; d_{calcd} = 1.76 g/cm^3 for Z = 2; anisotropic least-squares refinement converged at $R_1(F)$ = 7.3% and $R_2(F)$ = 8.9% for 737 independent reflections ($I > 2.0\sigma(I)$). $[(PPh_3)_2N]^+[Fe_2(\eta^5\text{-}C_5H_5)_2(\mu\text{-}NO)_2]^-$: M_r 840.19; triclinic; $P\bar{1}$; a = 11.266 (4) Å, b = 17.613 (4) Å, c = 10.362 (4) Å, α = 102.06 (3)°, β = 93.17 (3)°, γ = 92.06 (2)°, V = 2005 (1) Å^3 at T = 295 K; d_{calcd} = 1.39 g/cm^3 for Z = 2; anisotropic least-squares refinement for one independent cation and two independent half-anions of C_i—$\bar{1}$ site symmetries converged at $R_1(F)$ = 4.3% and $R_2(F)$ = 5.7% for 4174 independent reflections ($I > 2\sigma(I)$). $[Co_2(\eta^5\text{-}C_5H_4Me)_2(\mu\text{-}NO)_2]^+[PF_6]^-$: M_r 481.09; monoclinic; $C2/c$; a = 17.07 (1) Å, b = 7.530 (8) Å, c = 14.51 (1) Å, β = 113.51 (6)°; V = 1708 (3) Å^3 at T = 203 K; d_{calcd} = 1.87 g/cm^3 for Z = 4; anisotropic least-squares refinement converged at $R_1(F)$ = 8.5% and $R_2(F)$ = 10.7% for 1194 independent data ($I > 1.5\sigma(I)$).

Introduction

Our investigation of the physicochemical behavior of the 32-electron $Fe_2(\eta^5\text{-}C_5R_5)_2(\mu\text{-}NO)_2$ dimers, which formally possess an Fe–Fe double bond, was a consequence of earlier studies[2-6] which showed that the isoelectronic $Co_2(\eta^5\text{-}C_5R_5)_2(\mu\text{-}CO)_2$ dimers (R = H,[2-5] Me[5,6]) are reversibly reduced to their respective monoanions. The instability of the neutral unsubstituted cyclopentadienyl cobalt dimer

(1) (a) Based in part on the Ph.D. thesis of K. A. Kubat-Martin at the University of Wisconsin—Madison, June, 1986. Present address: Los Alamos Scientific Laboratory, University of California, Los Alamos, NM 87545. (b) On sabbatical leave (June 1985–Dec 1985) at UW—Madison from the Department of Chemistry, Beloit College, Beloit, WI 53511.

(2) (a) Ilenda, C. S.; Schore, N. E.; Bergman, R. G. *J. Am. Chem. Soc.* **1976**, *98*, 255–256 (synthesis). (b) Schore, N. E.; Ilenda, C. S.; Bergman, R. G. *J. Am. Chem. Soc.* **1976**, *98*, 256–258 (synthesis and structure).

(3) Lee, W.-S.; Brintzinger, H. H. *J. Organomet. Chem.* **1977**, *127*, 87–92.

(4) (a) Ginsburg, R. E. Ph.D. Thesis, University of Wisconsin—Madison, 1978. (b) Ginsburg, R. E.; Dahl, L. F., unpublished results.

(5) (a) Cirjak, L. M.; Ginsburg, R. E.; Dahl, L. F. *Inorg. Chem.* **1982**, *21*, 940–957. (b) Ginsburg, R. E.; Cirjak, L. M.; Dahl, L. F. *J. Chem. Soc., Chem. Commun.* **1979**, 468–470.

(6) (a) Bailey, W. I., Jr.; Collins, D. M.; Cotton, F. A.; Baldwin, J. C.; Kaska, W. C. *J. Organomet. Chem.* **1979**, *165*, 373–381. (b) Schore, N. E. *J. Organomet. Chem.* **1979**, *173*, 301–316.

0276-7333/87/2306-2570$01.50/0

precluded attempts by us[4] and others[2,6a] to determine and compare its structure with that of the structurally known monoanion[2,5] in order to assess the geometrical influence of the unpaired electron in the monoanion. This led to our synthesis and detailed structural-bonding analysis[5] of the corresponding pentamethylcyclopentadienyl $[Co_2(\eta^5\text{-}Me_5)_2(\mu\text{-}CO)_2]^n$ series (n = 0, 1-). The unpaired electron in the 33-electron monoanion was shown via "experimental quantum mechanics" to occupy the out-of-plane dimetal-antibonding π^* HOMO in agreement with theoretical predictions reported for the cyclopentadienyl analogues from extended Hückel calculations by Pinhas and Hoffmann[7] in 1979 and Bellagamba and Gamba[8] in 1981 and recently from MO calculations by Schugart and Fenske[9] via the Fenske–Hall method[10] in 1986.

Further experimental evidence that the unpaired electron in the 33-electron $[Co_2(\eta^5\text{-}C_5R_5)_2(\mu\text{-}CO)_2]^-$ monoanion occupies the out-of-plane dimetal antiboding π^* HOMO which lacks bridging ligand character was given by Connelly et al.[11] from their investigation of the electrochemical and relative reactivities of the $[Co_2(\eta^5\text{-}C_5R_5)_2(\mu\text{-}NO)_{2-x}(\mu\text{-}CO)_x]^n$ series (x = 0, R = H, Me, n = 0, 1+, 2+; x = 1, R = Me, n = 0, 1+); they found that an EPR spectrum of the closely related 33-electron $Co_2(\eta^5\text{-}C_5Me_5)_2(\mu\text{-}NO)(\mu\text{-}CO)$ exhibits an expected 15-line pattern due to a hyperfine interaction of the unpaired electron with both ^{59}Co nuclei (100% abundance, $I = {}^7/_2$) with no evidence of additional hyperfine coupling due to the bridging ^{14}N nuclei (99.63% abundance, I = 1). The proposed bonding model of Pinhas and Hoffmann[7] was also found to be consistent with a photoelectron (PE) study by Green and co-workers[12] in 1984 of the 32-electron $M_2(\eta^5\text{-}C_5Me_5)_2(\mu\text{-}CO)_2$ (M = Co, Rh), the 34-electron $Co_2(\eta^5\text{-}C_5Me_5)_2(\mu\text{-}NO)_2$, and the 33-electron $Co_2(\eta^5\text{-}C_5Me_5)_2(\mu\text{-}NO)(\mu\text{-}CO)$ and with a PE study by Ganzonni et al.[13] in 1982 of the 34-electron $Ni_2(\eta^5\text{-}C_5H_5)_2(\mu\text{-}CO)_2$.[14] The PE assignments were interpreted[12,13] in terms of delocalized bonding involving the dimetal-bridging ligand system in each dimer.

We presumed that the 32-electron $Fe_2(\eta^5\text{-}C_5H_5)_2(\mu\text{-}NO)_2$ (**1**), prepared by Brunner[15] in 1968 and structurally characterized by Day and co-workers[16] in 1974, would also undergo a reversible one-electron reduction. This hypothesis was substantiated by a cyclic voltammetric investigation, which in turn led to the isolation and the X-ray and EPR characterization[17] of the monoanion in order to determine the influence of the added unpaired electron. This 33-electron monoanion was also independently prepared and spectrally and electrochemically characterized as the sodium salt by Seidler and Bergman[18] in the course of their investigations of systems which might undergo migratory insertion of NO.

The recent synthesis by Diel[19] of $Fe_2(\eta^5\text{-}C_5Me_5)_2(\mu\text{-}NO)_2$ prompted our preparation of $Fe_2(\eta^5\text{-}C_5H_4Me)_2(\mu\text{-}NO)_2$ (**2**) in order to perform a systematic electrochemical study of the C_5H_5-, C_5H_4Me-, and C_5Me_5-containing iron dimers. An X-ray crystallographic investigation of the neutral methylcyclopentadienyl iron dimer was motivated by our desire to reduce the relatively large estimated standard deviations (esd's) of the molecular parameters reported in the X-ray diffraction study[16] of $Fe_2(\eta^5\text{-}C_5H_5)_2(\mu\text{-}NO)_2$. Unfortunately, our structural determination and refinement of the methylcyclopentadienyl iron dimer also yielded equally large esd's for the corresponding molecular parameters.

Pertinent to our investigation of these systems was a recent qualitative bonding analysis by Bottomley[20] in 1983 of dimeric transition-metal compounds containing π-acceptor bridging ligands. In his bonding assessment of the structural variations of a wide variety of nitrosyl- and carbonyl-bridged metal dimers, Bottomley[20] concluded that the metal–NO and metal–CO bond lengths (and hence the metal–metal distances) are dictated mainly by the degree of back-bonding from the filled metal orbitals to the empty NO or CO π^* acceptor orbitals. His generalization[20] that "the higher the energy of the metal atomic orbitals the shorter the metal–NO or metal–CO distance" was based upon the explanation by Cirjak, Ginsburg, and Dahl[5] that in the oxidation of the 33-electron $[Co_2(\eta^5\text{-}C_5Me_5)_2(\mu\text{-}CO)_2]^-$ monoanion to its 32-electron neutral parent the observed small *decrease* in the Co–Co distance "may be readily ascribed to the simultaneous *increase* in the lengths of the Co–CO bonds, which in being much stronger than the Co–Co interactions are the dominant factor in opposing any decrease in the Co–Co distance". The fact that the imposed symmetry of the dimetal-antibonding HOMO in the monoanion precludes any carbonyl orbital character for a planar $Co_2(CO)_2$ core led to their proposal[5] that the observed increase in the Co–CO bonds (upon oxidation of the monoanion) is due to a "loss of negative charge, which in turn lowers the metal AO's relative to the π^*(CO) symmetry orbitals and thereby decreases the d_π(M)–π^*(CO) back-bonding". Bottomley[20] pointed out that "with one exception, this rule appears to work well and explains for instance, why the mean Fe–NO distance of 1.77 Å in the 32-electron $Fe_2(\eta^5\text{-}C_5H_5)_2(\mu\text{-}NO)_2$[16] is less than the mean Co–CO distance of 1.825 Å in the 34-electron $Co_2(\eta^5\text{-}C_5H_5)_2(\mu\text{-}NO)_2$[21] despite the larger covalent radius of Fe compared to that of Co". He also stated that "the one exception is the *decrease* in the Co–NO distance on going from $Co_2(\eta^5\text{-}C_5H_5)_2(\mu\text{-}NO)_2$[21] to its $[Co_2(\eta^5\text{-}C_5H_5)_2(\mu\text{-}NO)_2]^+$ monocation (as the $[BF_4]^-$ salt)[22] for which there is no explanation".

During our investigation[23] of the redox chemistry of $Co_3(\eta^5\text{-}C_5H_4Me)_3(\mu_3\text{-}NO)_2$, we isolated the 33-electron $[Co_2(\eta^5\text{-}C_5H_4Me)_2(\mu\text{-}NO)_2]^+$ monocation as the $[PF_6]^-$ salt. In the hope of providing a reason for the indicated nonconformity of the $[Co_2(\eta^5\text{-}C_5H_5)_2(\mu\text{-}NO)_2]^n$ series (n = 0,

(7) Pinhas, A. R.; Hoffmann, R. *Inorg. Chem.* **1979**, *18*, 654–658.
(8) Bellagamba, V.; Gamba, A. *J. Organomet. Chem.* **1981**, *212*, 125–134.
(9) (a) Schugart, K. A.; Fenske, R. F. *J. Am. Chem. Soc.* **1986**, *108* 5094–5100. (b) Schugart, K. A.; Fenske, R. F. *J. Am. Chem. Soc.* **1986**, *108*, 5100–5104.
(10) Hall, M. B.; Fenske, R. F. *Inorg. Chem.* **1972**, *11*, 768–775.
(11) (a) Connelly, N. G.; Payne, J. D.; Geiger, W. E. *J. Chem. Soc., Dalton Trans.* **1983**, 295–299. (b) Clamp, S.; Connelly, N. G.; Payne, J. D. *J. Chem. Soc., Chem. Commun.* **1981**, 897–899.
(12) Dudeney, N.; Green, J. C.; Kirchner, O. N.; Smallwood, F. St. J. *J. Chem. Soc., Dalton Trans.* **1984**, 1883–1887.
(13) Granozzi, G.; Casarin, M.; Ajö, D.; Osella, D. *J. Chem. Soc., Dalton Trans.* **1982**, 2047–2049.
(14) (a) Byers, L. R.; Dahl, L. F. *Inorg. Chem.* **1980**, *19*, 680–692 and references contained therein. (b) Madach, T.; Fischer, K.; Vahrenkamp, H. *Chem. Ber.* **1980**, 113, 3235–3244.
(15) Brunner, H. *J. Organomet. Chem.* **1968**, *14*, 173–178.
(16) Calderõn, J. L.; Fontana, S.; Frauendorfer, E.; Day, V. W.; Iske, S. D. A. *J. Organomet. Chem.* **1974**, *64*, C16–C18.
(17) The electrochemical activity of $Fe_2(\eta^5\text{-}C_5H_5)_2(\mu\text{-}NO)_2$ and the structure of $[PPN]^+[Fe_2(\eta^5\text{-}C_5H_5)_2(\mu\text{-}NO)_2]^-$ have been previously reported; Kubat-Martin, K. A.; Rae, A. D.; Dahl, L. F. *Abstracts of Papers*, 187th National Meeting of the American Chemical Society, St Louis, MO; American Chemical Society: Washington, DC, 1984.
(18) Seidler, M. D.; Bergman, R. G. *Organometallics* **1983**, *2*, 1897–1899.
(19) Diel, B. N. *J. Organomet. Chem.* **1985**, *284*, 257–262.
(20) Bottomley, F. *Inorg. Chem.* **1983**, *22*, 2656–2660.
(21) Bernal, I.; Korp, J. D.; Reisner, G. M.; Herrmann, W. A. *J. Organomet. Chem.* **1977**, *139*, 321–336.
(22) Wochner, F.; Keller, E.; Brintzinger, H. H. *J. Organomet. Chem.* **1982**, *236*, 267–272.
(23) Kubat-Martin, K. A.; Rae, A. D.; Dahl, L. F. *Organometallics* **1985**, *4*, 2221–2223.

1+) to the expected change in Co–NO bond lengths upon oxidation from $n = 0$ to $n = 1+$, we performed X-ray crystallographic and EPR measurements on the dimeric methylcyclopentadienyl cobalt nitrosyl monocation. A resulting examination of the sizes, shapes, and orientations of the atomic thermal ellipsoids for the $Co_2(NO)_2$ cores in these dimers ($n = 0, 1+$) provides compelling evidence which accounts for the indicated noncompliance of the cobalt–nitrosyl series to the above-stated Bottomley rule.

Presented herein are (1) details of the synthesis and structural determination of $Fe_2(\eta^5\text{-}C_5H_4Me)_2(\mu\text{-}NO)_2$ (**2**), (2) an electrochemical investigation of the neutral $Fe_2(\eta^5\text{-}C_5H_{5-x}Me_x)_2(\mu\text{-}NO)_2$ dimers ($x = 0, 1, 5$), (3) the synthesis, spectroscopic-crystallographic characterization, and structural-bonding analysis of the $[Fe_2(\eta^5\text{-}C_5H_5)_2(\mu\text{-}NO)_2]^-$ monoanion (1^-), and (4) a stereochemical-bonding examination of the $[Co_2(\eta^5\text{-}C_5R_5)_2(\mu\text{-}NO)_2]^n$ series ($n = 0, 1+$).

In addition to this work, we also have shown[24,25] that cycloaddition of a 16-electron metal fragment to the 32-electron $Fe_2(\eta^5\text{-}C_5H_5)_2(\mu\text{-}NO)_2$ can occur to give a 48-electron triangular mixed-metal cluster containing a triply bridging nitrosyl ligand. This development of a preparative route to mixed-metal clusters containing triply bridging nitrosyl ligands was motivated by our previous success in utilizing the 32-electron $Co_2(\eta^5\text{-}C_5Me_5)_2(\mu\text{-}CO)_2$ in the rational synthesis of mixed-metal clusters via the photochemical addition of 16-electron metal fragments across the formal Co–Co double bond of the dimer to give 48-electron triangular metal clusters.[26]

Experimental Section

Materials and Measurements. All reactions, sample transfers, and sample manipulations were performed with oven-dried standard Schlenk-type glassware under nitrogen, either on a preparative vacuum line or within a Vacuum Atmospheres glovebox. The following solvents were dried and distilled immediately before use: THF (potassium–benzophenone), octane (CaH_2), toluene (sodium–benzophenone), CH_2Cl_2 (CaH_2), and hexane (CaH_2). $Fe_2(\eta^5\text{-}C_5H_5)_2(\mu\text{-}NO)_2$ and $Fe_2(\eta^5\text{-}C_5Me_5)_2(\mu\text{-}NO)_2$ were synthesized by the methods of Brunner[15] and Diel,[19] respectively. The potassium–benzophenone reducing agent was prepared by stirring benzophenone with an excess of potassium metal in THF. All other reagents were purchased from major chemical suppliers and were used without further purification.

Infrared spectra were recorded on a Beckman 4240 spectrophotometer, and NMR spectra were obtained with a Bruker WP-200 spectrometer. EPR measurements were obtained on a Varian E-15 spectrometer with DPPH used as a standard for g-value determinations. Glass samples were made by a quenching of dilute solutions in liquid N_2; low-temperature spectra were checked for possible power saturation. Cyclic voltammograms were obtained with a BAS-100 electrochemical analyzer with the electrochemical cell enclosed in a N_2-filled Vacuum Atmospheres glovebox.

Preparation and Physical Properties of $Fe_2(\eta^5\text{-}C_5H_4Me)_2(\mu\text{-}NO)_2$ (2). In a variation of the method of Brunner,[15] $Fe_2(\eta^5\text{-}C_5H_4Me)_2(CO)_2(\mu\text{-}CO)_2$ (4.11 g, 10.1 mmol) was refluxed in 150 mL of octane. Nitric oxide (1.2 L) was added to this stirred solution via syringe over a 2-h period. The octane was blown off under nitrogen, and the resulting product was washed with hexane, dissolved in a minimum amount of toluene, and then chromatographed on an alumina column which had been deoxygenated with degassed toluene. The dark green band eluted with toluene was identified from spectral data as **2** (2.70 g, 76% yield).

An infrared spectrum of **2** in THF exhibited a strong bridging nitrosyl peak at 1510 cm^{-1}. A ^1H NMR spectrum of **2** in $CDCl_3$ displayed two sets of cyclopentadienyl resonances at δ 4.68 (4 H) and 4.33 (4 H) and a single methyl proton resonance at δ 1.87 (6 H).

Cyclic Voltammetric Measurements of $Fe_2(\eta^5\text{-}C_5H_{5-x}Me_x)_2(\mu\text{-}NO)_2$ ($x = 0, 1, 5$). These measurements were carried out in THF/0.1 M $[NBu_4]^+[PF_6]^-$. The working electrode was a platinum disk; the reference electrode was a Vycor-tipped aqueous SCE separated from the test solution by a Vycor-tipped salt bridge filled with 0.1 M $TBAPF_6$ solution. The counter electrode was a platinum coil. Each solution consisted of ca. 5 mL of THF containing approximately 10^{-3} M dimer.

Preparation and Physical Properties of $[PPN]^+[Fe_2(\eta^5\text{-}C_5H_5)_2(\mu\text{-}NO)_2]^-$. $Fe_2(\eta^5\text{-}C_5H_5)_2(\mu\text{-}NO)_2$ (570 mg, 1.89 mmol) dissolved in ca. 50 mL of THF was added to a stirred suspension (1.10 g, 1.98 mmol) of $[PPN]^+[BH_4]^-$ in 25 mL of THF. The slurry was stirred for 2–3 h, after which the solution containing the monoanion (1^-) was filtered into a clean, dry flask and the THF was blown off under nitrogen. The small crystals that formed were washed with a hexane/toluene mixture (50/50) until the neutral dimer was no longer extracted (as evidenced by the absence of color in the washing solution). A yield of ca. 70% was obtained for this compound.

An infrared spectrum (KBr) of 1^- exhibited a bridging nitrosyl peak at 1395 cm^{-1}. Bands at 1480 and 1435 cm^{-1} were attributed to the $[PPN]^+$ counterion.

Preparation and Physical Properties of $[K(2,2,2\text{-crypt})]^+[Fe_2(\eta^5\text{-}C_5H_{5-x}Me_x)_2(\mu\text{-}NO)_2]^-$ ($x = 1, 5$). In a typical experiment the neutral dimer was mixed in a 1:1 molar ratio with 2,2,2-cryptand and then dissolved in 50 mL of THF. This solution was slowly titrated with a potassium–benzophenone THF solution until the bridging nitrosyl bands due to the starting material disappeared from the IR. The THF was removed under vacuum, and the resulting product was washed with dry, degassed toluene to remove excess benzophenone. Typical yields ranged from 50 to 60%. An infrared spectrum (THF) of the methylcyclopentadienyl iron monoanion exhibited a broad bridging nitrosyl band at 1380 cm^{-1}; an infrared spectrum (THF) of the pentamethylcyclopentadienyl iron monoanion displayed a bridging nitrosyl band at 1355 cm^{-1}.

EPR Spectrum of $[PPN]^+[Fe_2(\eta^5\text{-}C_5H_5)_2(\mu\text{-}NO)_2]^-$. A room-temperature solution EPR spectrum of the cyclopentadienyl iron monoanion in THF consisted of a single line at $g = 2.052$ (5) with a 15-G line width which narrowed as the temperature was lowered. A glass spectrum at −110 °C exhibited three principal g values ($g_1 = 2.143$ (5), $g_2 = 2.021$ (5), $g_3 = 1.975$ (5)); the average g value of 2.05 agreed with the isotropic solution value. As the microwave power was reduced, hyperfine structure on the high-field peak became partially resolved ($A_3 = 4$ G with a line width of 3 G).

Preparation and Physical Properties of $[Co_2(\eta^5\text{-}C_5H_4Me)_2(\mu\text{-}NO)_2]^+[PF_6]^-$. This methylcyclopentadienyl cobalt monocation (3^+) was unexpectedly prepared by the oxidation of $Co_3(\eta^5\text{-}C_5H_4Me)_3(\mu_3\text{-}NO)_2$ with 1 equiv of $AgPF_6$. In a typical experiment, $Co_3(\eta^5\text{-}C_5H_4Me)_3(\mu_3\text{-}NO)_2$ (100 mg, 0.211 mmol) was dissolved in 50 mL of CH_2Cl_2 and was added to a stirred suspension of $AgPF_6$ in CH_2Cl_2. As the dimeric product was contaminated with another oxidized species (presumably the sought-after and as yet structurally uncharacterized 47-electron $[Co_3(\eta^5\text{-}C_5H_4Me)_3(\mu_3\text{-}NO)_2]^+$ monocation), subsequent preparations of the dimeric cobalt monocation involved oxidation of the neutral $Co_2(\eta^5\text{-}C_5H_4Me)_2(\mu\text{-}NO)_2$[27] with $AgPF_6$. The neutral dimer (100 mg, 0.297 mmol) was dissolved in 50 mL of CH_2Cl_2 and then added to an equimolar amount of $AgPF_6$. The solvent was removed under vacuum, and the resulting product was washed with toluene. Typical yields of the monocation ranged from 60 to 70%.

An infrared spectrum (CH_2Cl_2) of 3^+ showed a sharp bridging nitrosyl band at 1600 cm^{-1}. An EPR spectrum (CH_2Cl_2) at room temperature (Figure 1) consisted of 15 lines of varying intensities characteristic of coupling of an unpaired electron with two equivalent cobalt nuclei (100% abundance, $I = {}^7/_2$). Spectral

(24) Kubat-Martin, K. A.; Dahl, L. F. *Abstracts of Papers*, 190th National Meeting of the American Chemical Society, Chicago, IL; American Chemical Society: Washington, DC, 1985.
(25) Kubat-Martin, K. A.; Spencer, B.; Dahl, L. F. *Organometallics*, following paper in this issue.
(26) Cirjak, L. M.; Huang, J.-S.; Zhu, Z.-H.; Dahl, L. F. *J. Am. Chem. Soc.* **1980**, *102*, 6623–6626.
(27) $Co_2(\eta^5\text{-}C_5H_4Me)_2(\mu\text{-}NO)_2$ was prepared in an analogous fashion to the original Brunner synthesis of $Co_2(\eta^5\text{-}C_5H_5)_2(\mu\text{-}NO)_2$: Brunner, H. *J. Organomet. Chem.* **1968**, *12*, 517–522.

Table I. Crystal, Data-Collection, and Structural Refinement Parameters for $Fe_2(\eta^5\text{-}C_5H_4Me)_2(\mu\text{-}NO)_2$ (2), $[PPN]^+[Fe_2(\eta^5\text{-}C_5H_5)_2(\mu\text{-}NO)_2]^-$ ($[PPN]^+[1]^-$), and $[Co_2(\eta^5\text{-}C_5H_4Me)_2(\mu\text{-}NO)_2]^+[PF_6]^-$ ($[3]^+[PF_6]^-$)

	2	$[PPN]^+[1]^-$	$[3]^+[PF_6]^-$
	A. Crystal Parameters		
fw	329.95	840.19	481.09
cryst system	monoclinic	triclinic	monoclinic
cell const temp, K	233	295	203
a, b, c, Å	7.966 (4), 8.644 (2), 9.833 (4)	11.266 (4), 17.613 (4), 10.362 (4)	17.07 (1), 7.530 (8), 14.51 (1)
α, β, γ, deg	90, 113.36 (3), 90	102.06 (3), 93.17 (3), 92.06 (2)	90, 113.51 (6), 90
V, Å^3	621.6 (4)	2005 (1)	1708 (3)
space group	$C2/m$	$P\bar{1}$	$C2/c$
Z	2	2	4
d_{calcd}, g/cm^3	1.76	1.39	1.87
μ, cm^{-1}	23.3	8.4	21.0
	B. Data-Collection and Structural Refinement Parameters		
data-collection temp, K	233	295	203
radiatn	Mo K$\bar{\alpha}$	Mo K$\bar{\alpha}$	Mo K$\bar{\alpha}$
scan mode	$\theta/2\theta$	$\theta/2\theta$	$\theta/2\theta$
scan speed, deg/min	variable (3–30)	variable (2–24)	variable 2–24)
scan range, deg above $K\alpha_1$/below $K\alpha_2$	1.0/1.0	1.0/1.0	1.0/1.0
2θ limits, deg	4.0–58.0	3.0–50.0	3.0–55.0
std reflctns	205; $\bar{3}\bar{3}3$; $1\bar{1}1$	$\bar{1}22$; $04\bar{2}$	$\bar{1}\bar{1}\bar{1}$; $\bar{3}\bar{1}3$; $\bar{4}1\bar{4}$
freq of stds	3/47	2/48	3/47
no. of independent data	1381	5799	1531
cutoff obsd data	$I > 2\sigma(I)$	$I > 2\sigma(I)$	$I > 1.5\sigma(I)$
no. of obsd data	737	4714	1194
data/parameter ratio	15.0/1	20.5/1	13.3/1
$R_1(F)$, $R_2(F)$, %	7.3, 8.9	4.4, 5.7	8.4, 10.7
goodness-of-fit	2.52	1.49	1.85

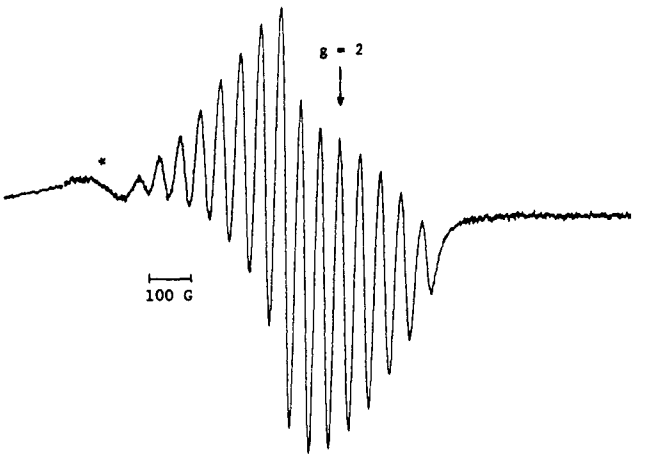

Figure 1. X-Band EPR spectrum of $[Co_2(\eta^5\text{-}C_5H_4Me)_2(\mu\text{-}NO)_2]^+[PF_6]^-$ in CH_2Cl_2 at room temperature with $g = 2.068$ (5) and $A = 43.4$ (5) G. In addition to the principal 15-line spectrum from coupling of the unpaired electron to two equivalent cobalt nuclei ($I = {}^7/_2$, 100% abundance) in the monocation, a less intense signal of greater line width from an unidentified paramagnetic impurity is also evident at the low-field end of the spectrum (*).

parameters are $g = 2.068$ (5) and $A = 43.4$ G with line widths varying from 19 to 26 G among hyperfine components.

Structural Determinations of $Fe_2(\eta^5\text{-}C_5H_4Me)_2(\mu\text{-}NO)_2$ (2), $[PPN]^+[Fe_2(\eta^5\text{-}C_5H_5)_2(\mu\text{-}NO)_2]^-$ ($[PPN]^+[1]^-$), and $[Co_2(\eta^5\text{-}C_5H_4Me)_2(\mu\text{-}NO)_2]^+[PF_6]^-$ ($[3]^+[PF_6]^-$). (a) General. Intensity data for each of the three compounds were collected with graphite-monochromatized Mo Kα radiation on a refurbished Nicolet diffractometer (upgraded from a P$\bar{1}$ to a P3F model). The procedures involved in crystal alignment and data collection are described elsewhere.[28] Crystal data, data-collection parameters, and final refinement parameters for each structure are presented in Table I. The quoted cell dimensions and esd's were obtained from least-squares analysis of setting angles for 15–25 well-centered, high-angle reflections. The intensities of the chosen standard reflections for each crystal (Table I) did not vary significantly during data collection. Atomic scattering factors for neutral atoms were used together with anomalous dispersion corrections for all non-hydrogen atoms.

Table II. Atomic Coordinates (×10^4) and Equivalent Isotropic Thermal Parameters[a] (Å^2 × 10^3) for $Fe_2(\eta^5\text{-}C_5H_5Me)_2(\mu\text{-}NO)_2$ (2)

	x	y	z	U
Fe	373 (2)	5000	8970 (2)	33
O	3394 (12)	5000	11644 (10)	59
N	1820 (13)	5000	10941 (10)	38
C(1)	−573 (18)	5000	6630 (13)	54
C(2)	509 (14)	3683 (11)	7230 (10)	54
C(3)	2259 (13)	4221 (12)	8176 (10)	57
Me	−2537 (22)	5000	5567 (15)	75

[a] The equivalent isotropic U is defined as one-third the trace of the orthogonalized U_{ij} tensor.

(b) $Fe_2(\eta^5\text{-}C_5H_4Me)_2(\mu\text{-}NO)_2$. Crystals were grown by slow evaporation of a THF solution (via vapor diffusion into toluene) of the dimer. A dark green parallelepiped-shaped crystal of dimensions 0.25 × 0.23 × 0.20 mm was mounted inside a thin-walled glass capillary which was evacuated, filled with argon, and then flame-sealed. Axial photographs verified the dimensions and symmetry of the chosen monoclinic unit cell. Systematic absences of hkl for $h + k$ odd indicated three probable monoclinic space groups: $C2$ (C_2^3, No. 5), Cm (C_s^3, No. 8), and $C2/m$ (C_{2h}^3, No. 12); our choice of the centrosymmetric space group $C2/m$, which was based upon the derived $|E|$'s indicating a centrosymmetric distribution, necessitates that each molecule possess C_{2h}—$2/m$ site symmetry. Attempts to refine the structure under each of the other two noncentrosymmetric space groups led to convergence with much higher esd's. A Patterson function was used to locate the independent iron atom under $C2/m$ symmetry. The other non-hydrogen atoms were located from difference Fourier syntheses coupled with least-squares refinement.[29] An empirical ψ-scan absorption correction was applied to the intensity data. Least-squares refinement included fixed contributions from the hydrogen atoms whose idealized positions (with C–H distances of 0.96 Å) were dependent on those of their respective coordinated carbon atoms. A final difference map did not reveal any residual electron densities indicative either of crystal disorder or the presence of a solvent molecule.

(28) Byers, L. R.; Dahl, L. F. *Inorg. Chem.* **1980**, *19*, 277–284.

(29) Programs used were those of SHELXTL (1984 version). Computations were performed on an Eclipse S/4 system.

Table III. Selected Distances and Bond Angles for $Fe_2(\eta^5\text{-}C_5H_4Me)_2(\mu\text{-}NO)_2$ (2)

	Distances (Å)		
Fe–Fe′	2.326 (4)	C(1)–C(2)	1.41 (1)
Fe–N	1.82 (1)	C(2)–C(3)	1.41 (1)
Fe–N′	1.78 (1)	C(3)–C(3a)	1.35 (2)
N–O	1.17 (1)		
Fe–C(1)	2.12 (1)	C(1)–Me	1.50 (2)
Fe–C(2)	2.09 (1)		
Fe–C(3)	2.06 (1)		
	Bond Angles (deg)		
Fe–N–Fe′	80.4 (4)	C(2)–C(1)–Me	126.1 (5)
N–Fe–N′	99.6 (4)	C(2)–C(3)–C(3a)	109.2 (5)
Fe–N–O	135.2 (11)	C(2)–C(1)–C(2a)	107.8 (10)
Fe′–N–O	144.4 (10)	C(1)–C(2)–C(3)	106.8 (8)

Coordinates for the nonhydrogen atoms from the last least-squares cycle are listed in Table II. Selected interatomic distances and bond angles are presented in Table III. Tables of coordinates for the hydrogen atoms and temperature parameters for all atoms along with a list of observed and calculated structure factor amplitudes are available as supplementary material.

(c) $[PPN]^+[Fe_2(\eta^5\text{-}C_5H_5)_2(\mu\text{-}NO)_2]^-$. Crystals suitable for X-ray diffraction were grown by the slow diffusion of hexane into a THF solution containing the compound. A large dark red crystal of approximate dimensions 2.0 × 1.0 × 1.5 mm was cleaved in order to obtain a parallelepiped-shaped crystal (0.7 × 0.5 × 0.5 mm). This crystal was mounted inside an argon-filled thin-walled glass capillary which was then flame-sealed. Axial photographs were used to verify the dimensions of the chosen triclinic cell. The crystal structure was determined by direct methods (MULTAN[30]) and refined by least-squares refinement (RAELS[31a]). An empirical absorption correction[31,32] was carried out. The cyclopentadienyl rings were constrained to regular pentagonal symmetry with C–C distances of 1.395 Å, and hydrogen atoms were inserted at idealized positions with fixed temperature parameters.[33] The choice of the centrosymmetric space group $P\bar{1}$ (C_i^1—No. 2) was substantiated by the successful refinement of the structure. A final difference map did not reveal any anomalous features.

Coordinates for the non-hydrogen atoms obtained from the last least-squares cycle are listed in Table IV. Selected interatomic distances and bond angles are given in Table V. Tables of coordinates for the hydrogen atoms and temperature parameters for all atoms and a listing of observed and calculated structure factor amplitudes are available as supplementary material.

(d) $[Co_2(\eta^5\text{-}C_5H_4Me)_2(\mu\text{-}NO)_2]^+[PF_6]^-$. Crystals were grown by slow diffusion of hexane into a CH_2Cl_2 solution containing the compound. A dark purple parallelepiped-shaped crystal (0.2 × 0.2 × 0.3 mm) was mounted inside an argon-filled thin-walled glass capillary which was then flame-sealed. Axial photographs substantiated the dimensions and symmetry of the chosen monoclinic cell. Systematic absences of hkl for $h + k$ odd and of $h0l$ for l odd indicated the probable monoclinic space groups to be $C2/c$ (C_{2h}^6—No. 15) or Cc (C_4^5—No. 9). Our choice of the centrosymmetric $C2/c$ space group, which was based upon the $|E|$'s conforming to a centrosymmetric distribution, results in each monocation possessing crystallographic C_i–$\bar{1}$ site symmetry and each $[PF_6]^-$ anion possessing C_2–2 site symmetry. An attempt to refine the structure under the noncentrosymmetric Cc symmetry led to convergence with higher esd's. The crystal structure was determined by the use of MULTAN[30] and was refined by the use of SHELXTL.[29] An empirical absorption correction was performed.[32] Crystal disorders involving two half-weighted orientations of the independent methylcyclopentadienyl ring and two half-weighted positions for the oxygen atom of the independent nitrosyl ligand were modeled with isotropic thermal parameters;

Table IV. Atomic Coordinates (×10⁴) and Equivalent Isotropic Thermal Parameters[a] (Å² × 10³) for $[PPN]^+[Fe_2(\eta^5\text{-}C_5H_5)_2(\mu\text{-}NO)_2]^-$

	x	y	z	U
	A. Monoanion (1^-)			
Fe(1)	4674 (5)	5619 (3)	4891 (6)	46 (0)
Fe(2)	5462 (5)	632 (4)	145 (6)	49 (0)
N(1)	4296 (3)	4996 (2)	5968 (3)	48 (1)
O(1)	3630 (3)	5001 (2)	6893 (3)	67 (1)
N(2)	5448 (3)	−53 (2)	1173 (4)	53 (1)
O(2)	5870 (3)	−119 (2)	2286 (4)	75 (1)
C(11)	4926 (4)	6853 (2)	5463 (5)	91 (2)
C(12)	3833 (5)	6626 (3)	5779 (5)	105 (2)
C(13)	3204 (3)	6276 (2)	4639 (7)	118 (2)
C(14)	3908 (6)	6287 (2)	3619 (4)	113 (2)
C(15)	4972 (4)	6644 (3)	4128 (6)	96 (2)
C(21)	7057 (3)	1312 (2)	457 (6)	98 (2)
C(22)	6528 (4)	1376 (2)	−725 (4)	92 (2)
C(23)	5469 (4)	1709 (2)	−493 (5)	91 (2)
C(24)	5344 (4)	1852 (2)	832 (5)	96 (2)
C(25)	6325 (5)	1607 (3)	1419 (4)	101 (2)
	B. $[PPN]^+$ Monocation			
N	1087 (3)	2820 (2)	7059 (3)	45 (1)
P(1)	874 (1)	2742 (1)	8517 (1)	37 (0)
P(2)	761 (1)	2444 (1)	5570 (1)	37 (0)
C(1A)	2124 (2)	3230 (2)	9535 (2)	42 (1)
C(1B)	2200 (3)	3284 (2)	10890 (3)	57 (1)
C(1C)	3164 (3)	3670 (2)	11657 (3)	72 (1)
C(1D)	4054 (3)	4003 (2)	11082 (3)	78 (1)
C(1E)	3992 (3)	3954 (2)	9743 (3)	86 (1)
C(1F)	3032 (3)	3569 (2)	8968 (2)	65 (1)
C(1G)	736 (2)	1744 (1)	8693 (3)	41 (1)
C(1H)	−290 (2)	1297 (2)	8198 (3)	51 (1)
C(1I)	−351 (3)	513 (2)	8183 (3)	63 (3)
C(1J)	603 (3)	170 (2)	8658 (3)	67 (3)
C(1K)	1624 (3)	605 (2)	9151 (3)	67 (2)
C(1L)	1694 (2)	1389 (2)	9170 (3)	54 (1)
C(1M)	−425 (2)	3240 (2)	9115 (3)	42 (1)
C(1N)	−556 (3)	3978 (2)	8877 (3)	61 (1)
C(1O)	1510 (3)	4401 (2)	9333 (4)	77 (1)
C(1P)	−2336 (3)	4092 (2)	10026 (3)	71 (1)
C(1Q)	−2218 (2)	3362 (2)	10268 (3)	73 (1)
C(1R)	−1267 (3)	2935 (2)	9816 (3)	60 (1)
C(2A)	634 (2)	3217 (2)	4702 (3)	43 (1)
C(2B)	−303 (3)	3267 (2)	3805 (3)	61 (1)
C(2C)	−359 (3)	3896 (2)	3211 (3)	77 (1)
C(2D)	515 (3)	4478 (2)	3506 (3)	77 (1)
C(2E)	1447 (3)	4438 (2)	4391 (4)	77 (2)
C(2F)	1510 (2)	3810 (2)	4990 (3)	60 (1)
C(2G)	1934 (2)	1857 (2)	4880 (2)	41 (1)
C(2H)	2725 (3)	1562 (2)	5698 (2)	54 (1)
C(2I)	3615 (3)	1100 (2)	5172 (3)	69 (1)
C(2J)	3723 (3)	930 (2)	3833 (3)	72 (1)
C(2K)	2947 (3)	1218 (2)	3011 (3)	71 (1)
C(2L)	2054 (3)	1680 (2)	3528 (3)	55 (1)
C(2M)	−605 (2)	1858 (2)	5281 (3)	43 (1)
C(2N)	−1635 (2)	2198 (1)	5733 (3)	52 (1)
C(2O)	−2697 (2)	1766 (2)	5571 (3)	64 (3)
C(2P)	−2741 (3)	996 (2)	4959 (3)	71 (5)
C(2Q)	−1729 (3)	651 (2)	4507 (3)	78 (5)
C(2R)	−663 (2)	1078 (2)	4665 (3)	62 (3)

[a] The equivalent isotropic U is defined as one-third the trace of the orthogonalized U_{ij} tensor.

(30) Germain, G.; Main, P.; Woolfson, M. M. *Acta Crystallogr., Sect. A: Cryst. Phys., Diffr., Theor. Gen. Crystallogr.* **1971**, A27, 368–376.

(31) (a) Rae, A. D. RAELS, A Comprehensive Least-Squares Program; University of New South Wales: Kensington, 1976; adapted for a Harris/7 computer by A. D. Rae, University of Wisconsin—Madison, 1984. (b) An absorption tensor is computed from the ΔF values by the use of an option in the program RAELS. This correction is similar to the one used by Höpe.[32]

(32) Höpe, H., personal communication (Feb 1984) to L. F. Dahl. The Höpe program ABSORPTION (Höpe, H.; Moezzi, B., unpublished results) utilizes an empirical absorption tensor from an expression relating $|F_o|$ and $|F_c|$.

(33) Although the hydrogen atoms are placed in idealized positions, RAELS[31a] reports esd's for these atoms. These estimates reflect the errors associated with the orientation of the local axial systems (calculated from the crystallographic coordinates of the ring carbon atoms) and not esd's of the fractional coordinates of these atoms. Likewise, the thermal factors and associated esd's reported for the hydrogen atoms are not meant to imply that these parameters have been determined accurately for this structure. These values arise from the calculation of the libration-like thermal motion of the rigid η^5-C_5H_5 group. Hydrogen atoms in their idealized positions are included in this calculation.

Table V. Selected Distances and Bond Angles for $[PPN]^+[Fe_2(\eta^5\text{-}C_5H_5)_2(\mu\text{-}NO)_2]^-$

A. Monoanion (1^-)

Distances (Å)

Fe(1)–Fe(1′)	2.377 (1)	Fe(1)–C(11)	2.134 (4)
Fe(1)–N(1)	1.778 (4)	Fe(1)–C(12)	2.103 (4)
Fe(1)–N(1′)	1.764 (3)	Fe(1)–C(13)	2.089 (4)
N(1)–O(1)	1.248 (4)	Fe(1)–C(14)	2.112 (4)
Fe(2)–Fe(2′)	2.378 (1)	Fe(1)–C(15)	2.140 (4)
Fe(2)–N(2)	1.770 (4)		2.116 (av)
Fe(2)–N(2′)	1.773 (4)		
N(2)–O(2)	1.253 (5)	Fe(2)–C(21)	2.095 (4)
		Fe(2)–C(22)	2.114 (4)
		Fe(2)–C(23)	2.134 (4)
		Fe(2)–C(24)	2.128 (4)
		Fe(2)–C(25)	2.104 (4)
			2.117 (av)

Bond Angles (deg)

Fe(1)–N(1)–Fe(1′)	84.3 (2)	Fe(2)–N(2)–Fe(2′)	84.3 (2)
N(1)–Fe(1)–N(1′)	95.7 (2)	N(2)–Fe(2)–N(2′)	95.7 (2)
Fe(1)–N(1)–O(1)	135.7 (3)	Fe(2)–N(2)–O(2)	138.9 (3)
O(1)–N(1)–Fe(1′)	138.2 (3)	O(2)–N(2)–Fe(2′)	136.8 (3)

$[PPN]^+$ Monocation

Distances (Å)

N–P(1)	1.575 (3)	P(1)–C(1M)	1.806 (3)
N–P(2)	1.565 (3)	P(2)–C(2A)	1.788 (3)
P(1)–C(1A)	1.790 (3)	P(2)–C(2G)	1.795 (3)
P(1)–C(1G)	1.807 (3)	P(2)–C(2M)	1.797 (3)

Bond Angles (deg)

P(1)–N–P(2)	143.6 (2)	N–P(2)–C(2A)	107.4 (2)
N–P(1)–C(1A)	106.7 (2)	N–P(2)–C(2G)	110.6 (2)
N–P(1)–C(1G)	113.0 (2)	N–P(2)–C(2M)	114.1 (2)
N–P(1)–C(1M)	111.4 (2)		

Table VI. Atomic Coordinates ($\times 10^4$) and Equivalent Isotropic Thermal Parameters[a] ($Å^2 \times 10^3$) for the Non-Hydrogen Atoms in $[Co_2(\eta^5\text{-}C_5H_4Me)_2(\mu\text{-}NO)_2]^+[PF_6]^-$

	x	y	z	U
A. Monocation (3^+)				
Co	600 (1)	808 (2)	5033 (1)	43 (1)
N	−509 (5)	1169 (11)	4360 (7)	55 (4)
O(1)	−953 (11)	2098 (33)	2646 (26)	63 (7)
O(2)	−989 (10)	2487 (33)	3975 (24)	56 (8)
C(1)	1735 (11)	762 (19)	4799 (15)	60 (5)
C(2)	1169	2046	4159	52 (5)
C(3)	1000	3330	4772	46 (4)
C(4)	1461	2839	5791	50
C(5)	1916	1251	5808	50
Me	2438 (18)	373 (36)	6769 (22)	91 (9)
C(1′)	1414 (13)	1314 (27)	4291 (10)	38 (5)
C(2′)	1075	2928	4482	54 (6)
C(3′)	1348	3109	5538	50
C(4′)	1855	1606	6001	50
C(5′)	1896	496	5230	56 (6)
Me′	2353 (25)	−1217 (51)	5238 (31)	108 (13)
B. $[PF_6]^-$ Monoanion				
P	000	2905 (5)	7500	57 (2)
F(1)	596 (7)	4394 (12)	7411 (7)	126 (6)
F(2)	473 (5)	2894 (10)	8686 (5)	93 (4)
F(3)	609 (6)	1414 (12)	7425 (7)	118 (5)

[a] The equivalent isotropic U is defined as one-third the trace of the orthogonalized U_{ij} tensor.

the other non-hydrogen atoms were refined anisotropically. Carbon–carbon distances within the C_5H_4Me ring were fixed to 1.420 Å, and hydrogen atoms inserted at idealized positions were included in the refinement as fixed-atom contributors. A final difference map did not indicate residual electron densities indicative either of further disorder or of a solvent molecule.

Atomic coordinates of the non-hydrogen atoms obtained from the output of the last least-squares cycle are given in Table VI. Selected interatomic distances and bond angles are presented in Table VII. Tables of coordinates for the hydrogen atoms and temperature parameters for all atoms along with a listing of observed and calculated structure factor amplitudes are available as supplementary material.

Table VII. Selected Distances and Bond Angles for $[Co_2(\eta^5\text{-}C_5H_4Me)_2(\mu\text{-}NO)_2]^+[PF_6]^-$

A. Monocation (3^+)

Distances (Å)

Co–Co	2.352 (3)	Co–C(1′)	2.10 (2)
Co–N	1.771 (8)	Co–C(2′)	2.09 (2)
Co–N′	1.768 (9)	Co–C(3′)	2.10 (2)
N–O(1)	1.23 (3)	Co–C(4′)	2.13 (2)
N–O(2)	1.27 (2)	Co–C(5′)	2.13 (3)
			2.11 (av)
Co–C(1)	2.10 (2)	C(5)–Me	1.48 (3)
Co–C(2)	2.10 (2)	C(5′)–Me′	1.51 (5)
Co–C(3)	2.10 (2)		
Co–C(4)	2.10 (2)		
Co–C(5)	2.10 (2)		
	2.10 (av)		

Bond Angles (deg)

Co–N–Co′	83.3 (3)	O(1)–N–Co′	138.8 (11)
N–Co–Co′	48.3 (3)	O(2)–N–Co′	135.1 (14)
N–Co–N′	96.7 (3)	C(4)–C(5)–Me	120.8 (15)
Co–N–O(1)	135.7 (14)	C(1)–C(5)–Me	131.1 (14)
Co–N–O(2)	136.4 (11)	C(1′)–C(5′)–Me′	118.6 (17)
		C(4′)–C(5′)–Me′	133.4 (16)

$[PF_6]^-$ Monoanion

Distances (Å)

P–F(1)	1.55 (1)	P–F(3)	1.56 (1)
P–F(2)	1.58 (1)		

Bond Angles (deg)

F(1)–P–F(2)	91.6 (5)	F(1)–P–F(3)	92.1 (6)
F(2)–P–F(3)	90.4 (5)		

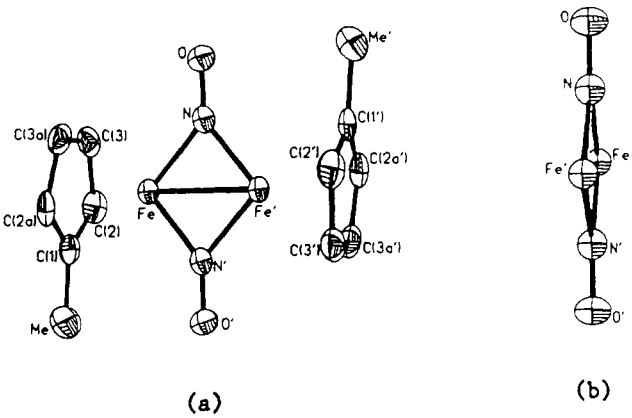

Figure 2. Two views of the molecular configuration of the methylcyclopentadienyl iron nitrosyl dimer $Fe_2(\eta^5\text{-}C_5H_4Me)_2(\mu\text{-}NO)_2$ (**2**), which possesses crystallographic C_{2h}—$2/m$ site symmetry. The principal twofold axis is perpendicular to the planar $Fe_2(NO)_2$ core which lies on the horizontal mirror plane. In view b of the $Fe_2(NO)_2$ core, the C_5H_4Me ligands are omitted for clarity. All atomic thermal ellipsoids are drawn at the 50% probability level.

Results and Discussion

Structural Description of $Fe_2(\eta^5\text{-}C_5H_4Me)_2(\mu\text{-}NO)_2$ (2). Figure 2 shows the solid-state configuration of **2**. The crystallographic C_{2h}—$2/m$ site symmetry necessitates that the molecule possess a planar $Fe_2(NO)_2$ core. The Fe–Fe distance of 2.326 (4) Å is the same as the Fe–Fe distance of 2.326 (4) Å found in $Fe_2(\eta^5\text{-}C_5H_5)_2(\mu\text{-}NO)_2$.[16] Unfortunately, the esd's are too large to ascertain whether a formal replacement of the C_5H_5 ligands with C_5H_4Me ligands gives rise to an indicated asymmetry in the linkage of each bridging nitrosyl group with the two iron atoms. In the *isostructural* 34-electron $Ni_2(\eta^5\text{-}C_5H_4Me)_2(\mu\text{-}CO)_2$,[14a] of crystallographic C_{2h}—$2/m$ site symmetry, the unsymme-

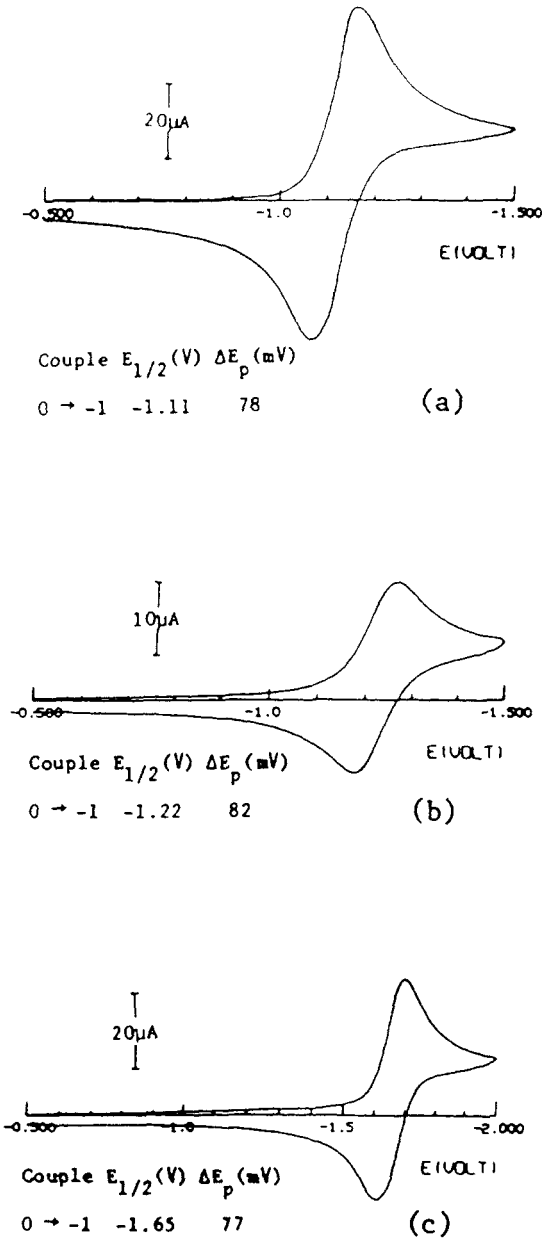

Figure 3. Cyclic voltammograms of (a) $Fe_2(\eta^5\text{-}C_5H_5)_2(\mu\text{-}NO)_2$, (b) $Fe_2(\eta^5\text{-}C_5H_4Me)_2(\mu\text{-}NO)_2$, and (c) $Fe_2(\eta^5\text{-}C_5Me_5)_2(\mu\text{-}NO)_2$. Each CV was carried out in THF/0.1 M $[NBu_4]^+[PF_6]^-$ at a platinum disk electrode with a scan rate of 200 mV/s.

trical ring orientations of the methylcyclopentadienyl ligands produce nonequivalent Ni–CO bond lengths; the Ni–CO bond trans to the methyl substituent is 0.05 Å longer than the Ni–CO bond cis to the methyl group. The two independent Fe–NO bond lengths of 1.82 (1) and 1.78 (1) Å in **2** are statistically comparable with those in $Fe_2(\eta^5\text{-}C_5H_5)_2(\mu\text{-}NO)_2$[16] (1.77 Å (av)). The average Fe–C(ring) distance of 2.09 Å in **2** is identical with the average Fe–C(ring) distance of 2.09 Å found in $Fe_2(\eta^5\text{-}C_5H_5)_2(\mu\text{-}NO)_2$.[16]

Cyclic Voltammetric Measurements of $Fe_2(\eta^5\text{-}C_5H_{5-x}Me_x)_2(\mu\text{-}NO)_2$ (x = 0, 1, 5). Cyclic voltammograms (Figure 3) for these three neutral dimers exhibit reversible one-electron reduction couples with $E_{1/2}$ values of −1.11 V for x = 0, −1.22 V for x = 1, and −1.65 V for x = 5. For a 200 mV/s scan rate, the corresponding peak separations (viz., $E_{p,c} - E_{p,a}$) for x = 0, 1, and 5 are 78, 82, and 77 mV, respectively; prime evidence for chemical reversibility of the oxidation and reduction waves in each couple is given by the experimental equivalence between the anodic and cathodic peak currents. A comparative analysis of these $E_{1/2}$ values shows that the pentamethylcyclopentadienyl iron dimer has the highest negative $E_{1/2}$ value and, hence, is the most difficult one to reduce to its monoanion. Likewise, the methylcyclopentadienyl iron dimer is more difficult to reduce than the cyclopentadienyl iron dimer. This trend is consistent with the electron-donating ability of the cyclopentadienyl ligand being enhanced with an increased number of methyl substituents. As is also seen in the series $(\eta^5\text{-}C_5H_{5-x}Me_x)CoNi_2(\eta^5\text{-}C_5H_5)_2(\mu_3\text{-}CO)_2$ (x = 0, 1, 5),[34] there is a linear correlation between $E_{1/2}$ values and the number of methyl substituents on the $C_5H_{5-x}Me_x$ ring. One-fifth of the 0.54-mV separation between the $E_{1/2}$ values for x = 0 and x = 5 is equivalent to the 0.11-mV separation between the $E_{1/2}$ values for x = 0 and x = 1.

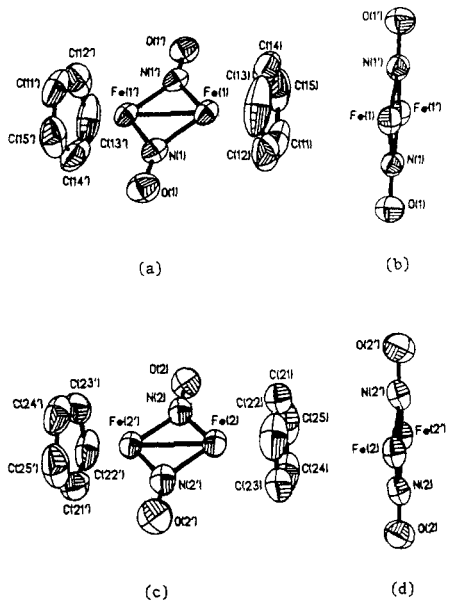

Figure 4. Two views of the configuration for each of the two independent half $[Fe_2(\eta^5\text{-}C_5H_5)_2(\mu\text{-}NO)_2]^-$ monoanions (1−) of crystallographic C_i—$\bar{1}$ site symmetry. In views b and d of the $Fe_2(NO)_2$ cores, the C_5H_5 ligands are omitted for clarity. All atomic thermal ellipsoids are drawn at the 50% probability level.

EPR and Structural Description of the $[Fe_2(\eta^5\text{-}C_5H_5)_2(\mu\text{-}NO)_2]^-$ Monoanion (1^-). A solution EPR spectrum of the monoanion is in accordance with EPR data reported by Seidler and Bergman.[18] The three principal g values of a glass spectrum at −110 °C are characteristic of a single unpaired electron in a C_{2h}—$2/m$ environment. The relatively narrow EPR resonance in solution and the small deviation of the g-values from that of the free electron are consistent with the unpaired electron occupying a nondegenerate orbital. The partially resolved hyperfine structure on the high-field peak is suggestive of coupling of the unpaired electron to two equivalent ^{14}N nuclei (99.63% abundance, I = 1) to yield a possible five-line spectrum, but lack of observable isotropic hyperfine structure in the solution spectrum (despite the narrow lines) and observation of possible nitrogen hyperfine on only one of the three components of the glass spectrum (presumably from a dipolar interaction with the nitrogen nuclei) suggest that the HOMO is primarily metal-based.

The solid-state structure of 1^- reinforces this view. The unit cell of $P\bar{1}$ symmetry contains two independent half anions with C_i—$\bar{1}$ site symmetry and one independent $[PPN]^+$ cation. Figure 4 shows the two independent half

(34) Byers, L. R.; Uchtman, V. A.; Dahl, L. F. *J. Am. Chem. Soc.* **1981**, *103*, 1942–1951.

Table VIII. Comparison of Mean Geometrical Parameters for the Carbonyl- and Nitrosyl-Bridged $[M_2(\eta^5\text{-}C_5R_5)_2(\mu\text{-}X)_2]^n$ Series Containing a M_2E_2 Core with Various C_5R_5 Ligands

dimer	cryst site symmetry	idealized M_2E_2 geometry	torsional angle of M_2E_2 core, deg	M–M′ bond order	M–M′, Å	M–E, Å	M–E–M′, deg	E–M–E, deg
$[Co_2Y_2(\mu\text{-}CO)_2]^n$								
Y = C_5Me_5; n = 0[a]	C_1—1	C_{2v} (bent)	176	2.0	2.338 (2)	1.858	78.4 (5)	101.6 (5)
Y = C_5Me_5; n = 1−[a,b]	C_1—1	C_{2v} (bent)	168	1.5	2.372 (1)	1.827	81.8 (3)	97.6 (3)
Y = C_5H_5; n = 1−[a,c]	C_i—$\bar{1}$	D_{2h} (planar)	180	1.5	2.364 (2)	1.815	81.3 (4)	98.7 (4)
Y = C_5H_5; n = 1−[d,e]	C_i—$\bar{1}$	D_{2h} (planar)	180	1.5	2.372 (2) 2.359 (2)	1.82	81.2 (5)	98.5 (5)
$[Fe_2Y_2(\mu\text{-}NO)_2]^n$								
Y = C_5H_4Me; n = 0[f]	C_{2h}—2/m	C_{2h} (planar)[g]	180	2.0	2.326 (4)	1.80[g]	80.4 (4)	99.6 (4)
Y = C_5H_5; n = 0[h]	C_i—$\bar{1}$	D_{2h} (planar)	180	2.0	2.326 (4)	1.77	82.3 (4)	97.7 (4)
Y = C_5H_5; n = 1−[e,f]	C_i—$\bar{1}$	D_{2h} (planar)	180	1.5	2.377 (1)	1.771	84.3 (2)	95.7 (2)
$[Co_2Y_2(\mu\text{-}NO)_2]^n$								
Y = C_5H_4Me; n = 1+[f,i]	C_i—$\bar{1}$	D_{2h} (planar)	180	1.5	2.352 (3)	1.77	83.3 (3)	96.7 (3)
Y = C_5H_5; n = 1+[j,k]	C_i—$\bar{1}$	D_{2h} (planar)	180	1.5	2.348 (5)	1.77	83 (1)	96 (2)
Y = C_5H_5; n = 0[l]	C_i—$\bar{1}$	D_{2h} (planar)	180	1.0	2.372 (1)	1.825	81.1 (3)	98.9 (3)

[a] Reference 5. [b] $[Na(2,2,2\text{-crypt})]^+$ salt. [c] $[AsPh_4]^+$ salt. [d] Reference 2. [e] $[PPN]^+$ salt. [f] This work. [g] The (μ-NO) bridge is asymmetric. [h] Reference 16. [i] $[PF_6]^-$ salt. [j] Reference 22. [k] $[BF_4]^-$ salt. [l] Reference 21.

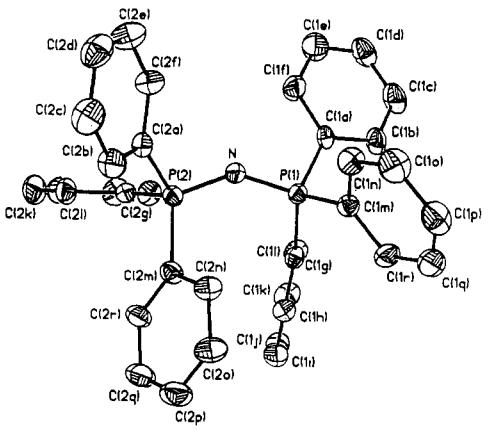

Figure 5. View of the configuration of the "bent" bis(triphenylphosphine)nitrogen(1+) monocation, $[PPN]^+$, drawn with atomic thermal ellipsoids at the 20% probability level.

monoanions 1^-. The $[PPN]^+$ counterion (Figure 5) exhibits the common "bent" geometry[35] rather than a "linear" geometry.[36]

Comparative Structural-Bonding Analysis of the Isoelectronic $[Fe_2(\eta^5\text{-}C_5H_5)_2(\mu\text{-}NO)_2]^-$ and $[Co_2(\eta^5\text{-}C_5H_5)_2(\mu\text{-}CO)_2]^-$ Monoanions. Table VIII lists the mean geometrical parameters for the 33-electron $[Fe_2(\eta^5\text{-}C_5H_5)_2(\mu\text{-}NO)_2]^-$ monoanion (isolated as the $[PPN]^+$ salt) and the 33-electron $[Co_2(\eta^5\text{-}C_5H_5)_2(\mu\text{-}CO)_2]^-$ monoanion which was structurally characterized both as the $[AsPh_4]^+$ salt[4,5] and as the $[PPN]^+$ salt.[2] In each of these structures a center of symmetry constrains the Fe_2N_2 or corresponding Co_2C_2 fragment to planarity.

The fact that the mean Fe–NO bond length of 1.771 Å in 1^- is 0.05 Å shorter than the mean Co–CO bond lengths of 1.82 Å in both salts of the cobalt monoanion is readily attributed to the much greater back-bonding ability of the bridging nitrosyl ligand compared to that of the bridging carbonyl ligand. On the other hand, the Fe–Fe distance of 2.377 (1) Å in 1^- is slightly longer than the Co–Co distance in the cobalt monoanion both as the $[AsPh_4]^+$ salt (2.364 (2) Å)[4,5] and as the $[PPN]^+$ salt (2.359 (2) and 2.372 (2) Å in the two independent half monoanions).[2]

Comparative Structural-Bonding Analysis within the 32/33-Electron $[Fe_2(\eta^5\text{-}C_5H_5)_2(\mu\text{-}NO)_2]^n$ Series (n = 0, 1−) and Resulting Electronic Implications. Upon oxidation of the 33-electron $[Fe_2(\eta^5\text{-}C_5H_5)_2(\mu\text{-}NO)_2]^-$ monoanion (1^-) to its neutral parent, the salient geometrical change (Table VIII) is that the Fe–Fe bond distance significantly decreases from 2.378 (1) (av) to 2.326 (4) Å. This 0.052-Å shortening of the Fe–Fe distance parallels the corresponding 0.034-Å shortening of the Co–Co distance upon oxidation of the 33-electron $[Co_2(\eta^5\text{-}C_5Me_5)_2(\mu\text{-}CO)_2]^-$ monoanion to its neutral parent. These similar bond-length variations, together with the EPR data for both the iron and cobalt monoanions, provide convincing evidence that the electronically equivalent $[Fe_2(\eta^5\text{-}C_5H_5)_2(\mu\text{-}NO)_2]^n$ and $[Co_2(\eta^5\text{-}C_5Me_5)_2(\mu\text{-}CO)_2]^n$ series (n = 0, 1−) have similar corresponding LUMO's (n = 0) and HOMO's (n = 1−). These results corroborate the unambiguous experimental assignment[5] of the unpaired electron in the $[Co_2(\eta^5\text{-}C_5Me_5)_2(\mu\text{-}CO)_2]^-$ monoanion to the HOMO containing mainly out-of-plane d_π dimetal-antibonding character in agreement with the earlier theoretical prediction by Pinhas and Hoffmann.[7] This experimental assignment is also in agreement with the recent MO calculations by Schugart and Fenske[9] using the nonparameterized Fenske–Hall method[10] on the 32/34-electron $M_2(\eta^5\text{-}C_5H_5)_2(\mu\text{-}NO)_2$ dimers (M = Fe, Co), the 32/34-electron $M_2(\eta^5\text{-}C_5H_5)_2(\mu\text{-}CO)_2$ dimers (M = Co, Ni), and the 32/33-electron $[Co_2(\eta^5\text{-}C_5H_5)_2(\mu\text{-}NO)(\mu\text{-}CO)]^n$ dimers (n = 1+, 0). Their results,[9] which indicated important bonding variations (directly related to molecular stabilities) between metal–(bridging nitrosyl) and metal–(bridging carbonyl) dimers, provided a theoretical basis for the earlier experimentally based arguments[12,20] that the molecular dimensions (including the metal–metal distances) of these dimers are primarily governed by the extent of delocalized metal–(bridging ligand) back-bonding.

In contrast to the $[Co_2(\eta^5\text{-}C_5Me_5)_2(\mu\text{-}CO)_2]^n$ series (n = 0, 1−) exhibiting a concomitant lengthening of the mean Co–CO bond length by 0.024 Å upon oxidation, the $[Fe_2(\eta^5\text{-}C_5H_5)_2(\mu\text{-}NO)_2]^n$ series (n = 0, 1−) shows no *detectable* lengthening of the mean Fe–NO bond length upon oxidation (i.e., the mean Fe–NO bond lengths are 1.77 Å in both 1^- and **1**). Upon oxidation, an increase in Fe–NO bond length would be expected on the basis that a decrease in d_π(Fe) to π^*(NO) back-bonding is the dominant electronic factor for this bond-lengthening (in accordance with

(35) (a) Ginsburg, R. E.; Berg, J. M.; Rothrock, R. K.; Collman, J. P.; Hodgson, K. O.; Dahl, L. F. *J. Am. Chem. Soc.* **1979**, *101*, 7218–7231. (b) Ruff, J. K.; White, R. P., Jr.; Dahl, L. F. *J. Am. Chem. Soc.* **1971**, *93*, 2159–2176. (c) Handy, L. B.; Ruff, J. K.; Dahl, L. F. *J. Am. Chem. Soc.* **1970**, *92*, 7327–7337.

(36) (a) Wilson, R. D.; Bau, R. *J. Am. Chem. Soc.* **1974**, *96*, 7601–7602. (b) Longoni, G.; Manassero, M.; Sansoni, M. *J. Organomet. Chem.* **1979**, *174*, C41–C44.

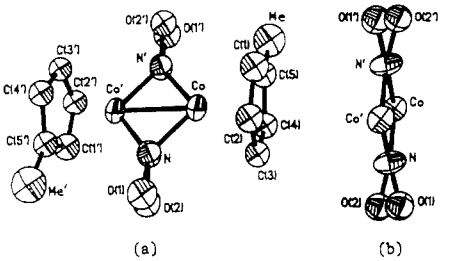

Figure 6. Two views of the configuration of the dimeric methylcyclopentadienyl cobalt nitrosyl monocation $[Co_2(\eta^5\text{-}C_5H_4Me)_2(\mu\text{-}NO)_2]^+$ (**3+**) of the $[PF_6]^-$ salt. The crystallographically imposed C_i—$\bar{1}$ site symmetry requires a planar Co_2N_2 fragment. Only one of the orientations is shown for the independent C_5H_4Me ligand which is randomly disordered between two noncentrosymmetrically related orientations. A crystal disorder of the independent bridging nitrosyl ligand in two nonplanar sites is evidenced by the resolution of two half-weighted out-of-plane thermal ellipsoids that are shown for the nitrosyl oxygen atom and by the abnormal out-of-plane elongation of the thermal ellipsoid for the nitrogen atom. The sizes, shapes, and orientations of these atomic thermal ellipsoids for the nitrosyl ligand strongly suggest a crystal disorder involving the superposition of two nonplanar conformations for the $Co_2(NO)_2$ core. All atomic thermal ellipsoids are drawn at the 50% probability level.

the Bottomley rule[20]). Spectral evidence for a significant decrease in back-bonding of the nitrosyl ligands in the oxidized neutral iron parent relative to that in the iron monoanion is given by the considerable increase in observed nitrosyl IR frequency from 1395 cm^{-1} in the monoanion to 1510 cm^{-1} in the neutral dimer. However the indicated *invariance* of the mean Fe–NO bond length upon removal of the unpaired electron from the out-of-plane dimetal-antibonding HOMO of the 33-electron monoanion may be readily attributed (at least in part) to the concurrent *decrease* in the Fe–Fe separation by 0.052 Å. Moreover, electronic considerations enable one to rationalize that a one-electron oxidation of the $[Fe_2(\eta^5\text{-}C_5H_5)_2(\mu\text{-}NO)_2]^-$ monoanion should lead to a considerably *smaller* and probably *nondiscernible increase* in the mean Fe–NO bond length relative to the observed 0.024 Å *increase* in the mean Co–CO bond length upon a one-electron oxidation of the corresponding $[Co_2(\eta^5\text{-}C_5Me_5)_2(\mu\text{-}CO)_2]^-$ monoanion. The intrinsically much stronger Fe–NO bonds than Co–CO bonds in the electronically equivalent cyclopentadienyl iron nitrosyl and cobalt carbonyl monoanions are reflected by the mean Fe–NO bond length being significantly shorter than the mean Co–CO bond length (vide supra). The stronger Fe–NO interactions are readily attributed to a much larger participation of the π^*(NO) orbitals in back-bonding due to the π^*(NO) orbitals being energetically lower and hence closer to the d_π(Fe) AO's than the π^*(CO) orbitals to the d_π(Co) AO's. It follows that the stronger Fe–NO bonds should undergo less bond-length increase than the considerably weaker Co–CO bonds upon decreased back-bonding due to oxidation.

Structural Description of the $[Co_2(\eta^5\text{-}C_5H_4Me)_2(\mu\text{-}NO)_2]^+$ Monocation (3^+). The solid-state structure of 3^+ (as the $[PF_6]^-$ salt) is shown in Figure 6. As in the isoelectronic $[Fe_2(\eta^5\text{-}C_5H_5)_2(\mu\text{-}NO)]^-$ monoanion (1^-), the crystallographic C_i—$\bar{1}$ site symmetry of 3^+ requires the Co_2N_2 fragment to be planar. The Co–Co distance of 2.352 (3) Å and the two independent Co–NO bond lengths of 1.768 (9) and 1.771 (8) Å in 3^+ compare favorably with the two identical Co–Co distances of 2.348 (5) Å and the four independent Co–NO distances of 1.77 (2), 1.77 (2), 1.75 (4), and 1.76 (3) Å in the two independent half $[Co_2(\eta^5\text{-}C_5H_5)_2(\mu\text{-}NO)_2]^+$ monocations of the $[BF_4]^-$ salt.[22]

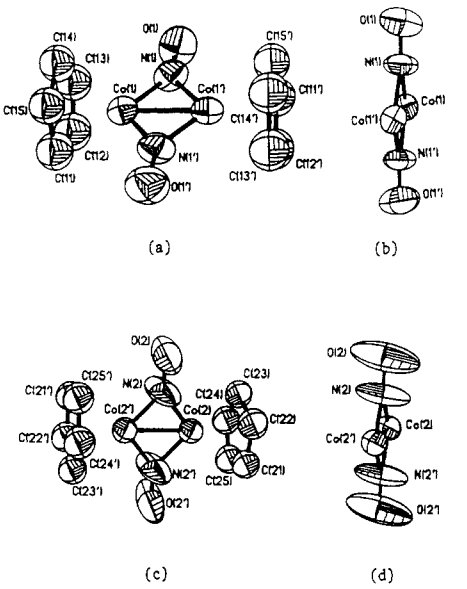

Figure 7. Two views of the previously determined configuration[22] for each of the two independent half $[Co_2(\eta^5\text{-}C_5H_5)_2(\mu\text{-}NO)_2]^+$ monocations of the $[BF_4]^-$ salt. The crystallographically imposed C_i—$\bar{1}$ site symmetry requires a planar Co_2N_2 fragment for each monocation. The abnormally elongated out-of-plane thermal ellipsoids for *both* the nitrogen and oxygen atoms in both monocations (shown in views b and d of the $Co_2(NO)_2$ cores) provides definitive evidence of a crystal disorder involving the superposition of at least two nonplanar orientations for each $Co_2(NO)_2$ core. All atomic thermal ellipsoids are drawn at the 50% probability level.

Comparative Structural-Bonding Analysis of the 34-Electron Neutral $Co_2(\eta^5\text{-}C_5H_5)_2(\mu\text{-}NO)_2$ and the 33-Electron $[Co_2(\eta^5\text{-}C_5H_{5-x}Me_x)_2(\mu\text{-}NO)_2]^+$ Monocations (x = 0, 1). From a systematic examination of the structural features of a large number of carbonyl- and nitrosyl-bridged dimers, Bottomley[20] concluded that the metal–CO or metal–NO bond lengths (and hence the metal–metal distances) are primarily governed by the extent of back-bonding from the filled metal orbitals to the empty π^*(CO) or π^*(NO) acceptor orbitals. He formulated a general rule that the higher the energy of the metal atomic orbitals, the shorter the metal–CO or metal–NO distance; hence, oxidation of a carbonyl- or nitrosyl-bridged dimer should (in general) give rise to *longer* metal–CO or metal–NO bond lengths. He pointed out that the only one exception to this rule is the $[Co_2(\eta^5\text{-}C_5H_5)_2(\mu\text{-}NO)_2]^n$ series (n = 0, 1+) where the mean Co–NO bond length (Table VIII) *decreases* upon oxidation of the neutral parent to its monocation.

Our interest in determining the reason for this theoretically inexplicable bond-length variation led to a structural determination of the corresponding $[Co_2(\eta^5\text{-}C_5H_4Me)_2(\mu\text{-}NO)_21^+$ monocation. A comparison (Table VIII) of its mean geometrical parameters with those of the C_5H_5-containing monocation showed the same mean Co–NO bond length of 1.77 Å which is 0.055 Å smaller than that of 1.825 Å in the neutral parent. The Co–Co distances of 2.352 (3) Å in the C_5H_4Me-containing monocation 3^+ and 2.348 (5) Å in the C_5H_5-containing monocation are 0.02 Å shorter than the Co–Co distance of 2.372 (1) Å in the 34-electron neutral C_5H_5-containing dimer. Hence, part of the indicated 0.055-Å decrease in the mean Co–NO bond length upon removal of an electron from the filled HOMO (which is largely composed of out-of-plane d_π dimetal-antibonding character) may be a consequence of the resulting small but significant 0.02-Å decrease in the Co–Co separation.

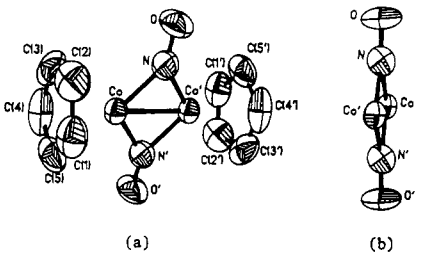

Figure 8. Two views of the previously determined configuration[21] of the neutral cyclopentadienyl cobalt nitrosyl dimer $Co_2(\eta^5\text{-}C_5H_5)_2(\mu\text{-}NO)_2$. The crystallographically imposed C_i—$\bar{1}$ site symmetry necessitates a planar Co_2N_2 fragment. In contrast to the monocations, the size, shape, and orientation of the thermal ellipsoid for the independent nitrosyl nitrogen atom appear to be normal. Hence, the elongated out-of-plane thermal ellipsoid for the nitrosyl oxygen atom may (in this case) be due to an anisotropic bending motion (expected to be considerably larger for the outer oxygen atom) rather than an indication of a crystal disorder. All atomic thermal ellipsoids are drawn at the 50% probability level.

The fact that in both cobalt monocations each of the bridging nitrosyl ligands possesses extremely large out-of-plane atomic thermal ellipsoids provided the insight that the calculated Co–NO distances correspond to an averaged (instead of an instantaneous) structure in which each bridging nitrosyl ligand occupies at least two bent orientations in the crystalline state. Figure 6b and parts b and d of Figure 7 depict side views along the Co–Co axis for the $[Co_2(\eta^5\text{-}C_5H_4Me)_2(\mu\text{-}NO)]^+$ monocation ($\mathbf{3}^+$) and for the two independent centrosymmetric $[Co_2(\eta^5\text{-}C_5H_5)_2(\mu\text{-}NO)_2]^+$ monocations. Figure 8 shows the $Co_2(\eta^5\text{-}C_5H_5)_2(\mu\text{-}NO)_2$ neutral dimer with a similar view down the Co–Co axis. In the case of the three centrosymmetric monocations (seen in Figures 6 and 7), the large out-of-plane thermal ellipsoids of the nitrogen and oxygen atoms (indicative of an averaged structure) are apparent. In contrast, the structure of the neutral $Co_2(\eta^5\text{-}C_5H_5)_2(\mu\text{-}NO)_2$ does not show these large out-of-plane ellipsoids and neither do the structures of **2** and $\mathbf{1}^-$ (Figure 2b and parts b and d of Figure 4, respectively). It is noteworthy that in the $[Ni_3(\eta^5\text{-}C_5H_5)_3(\mu\text{-}S)]_2(C_2S_4)$ molecule[37] the two ethylene carbon atoms exhibit extremely large out-of-plane thermal ellipsoids indicative of an averaged structure in which these carbon atoms occupy at least two orientations; this crystal disorder is reflected in an *artificially* shortened C–C distance of only 1.13 Å which is 0.2 Å shorter than the normal length. In an analogous fashion, the abnormally elongated thermal ellipsoids in the centrosymmetric cobalt monocations would also give rise to *artifically* shortened Co–NO distances vs that in the neutral dimer. Hence, the theoretically inexplicable shortening of the Co–NO bond lengths upon oxidation may be due primarily to an artifact arising from a crystal disorder of the nitrosyl ligands in the monocation of the $[Co_2(\eta^5\text{-}C_5H_5)_2(\mu\text{-}NO)_2]^n$ series (n = 0, 1+).

Acknowledgment. This research was generously supported by the National Science Foundation. We are especially grateful to Dr. Kimberly A. Schugart and Professor Richard F. Fenske for preprints of their publications and to Dr. Kenneth J. Haller for helpful crystallographic advice.

Registry No. $[PPN]^+[\mathbf{1}]^-$, 110487-89-3; **2**, 87597-79-3; $[\mathbf{3}]^+[PF_6]^-$, 110487-91-7; $Fe_2(\eta^5\text{-}C_5H_4Me)_2(CO)_2(\mu\text{-}CO)_2$, 32028-30-1; $Fe_2(\eta^5\text{-}C_5H_5)_2(\mu\text{-}NO)_2$, 52124-51-3; $Fe_2(\eta^5\text{-}C_5Me_5)_2(\mu\text{-}NO)_2$, 99030-99-6; $[K(2,2,2\text{-crypt})]^+[Fe_2(\eta^5\text{-}C_5H_4Me)_2(\mu\text{-}NO)_2]^-$, 110487-93-9; $[K(2,2,2\text{-crypt})]^+[Fe_2(\eta^5\text{-}C_5Me_5)_2(\mu\text{-}NO)_2]^-$, 110510-85-5; $Co_3(\eta^5\text{-}C_5H_4Me)_3(\mu_3\text{-}NO)_2$, 98689-82-8; $Co_2(\eta^5\text{-}C_5H_4Me)_2(\mu\text{-}NO)_2$, 85454-64-4; 2,2,2-cryptand, 23978-09-8.

Supplementary Material Available: Tables of the positions and thermal parameters for all atoms (6 pages); listings of observed and calculated structure factor amplitudes for $Fe_2(\eta^5\text{-}C_5H_4Me)_2(\mu\text{-}NO)_2$, $[PPN]^+[Fe_2(\eta^5\text{-}C_5H_5)_2(\mu\text{-}NO)_2]^-$, and $[Co_2(\eta^5\text{-}C_5H_4Me)_2(\mu\text{-}NO)_2]^+[PF_6]^-$ (51 pages). Ordering information is given on any current masthead page.

(37) Maj, J. J.; Rae, A. D.; Dahl, L. F. *J. Am. Chem. Soc.* **1982**, *104*, 4278–4280.